

# A Conformationally Stable $\pi$ -Expanded X-Type Double Helicene Comprising Dihydropyracylene Units with Multistage Redox Behavior

John Bergner,<sup>[a]</sup> Jan Borstelmann,<sup>[a]</sup> Luca M. Cavinato,<sup>[b]</sup> Juan Pablo Fuenzalida-Werner,<sup>[b]</sup> Christian Walla,<sup>[a, c]</sup> Heike Hinrichs,<sup>[d]</sup> Philipp Schulze,<sup>[d]</sup> Frank Rominger,<sup>[a]</sup> Rubén D. Costa,<sup>[b]</sup> Andreas Dreuw,<sup>[c]</sup> and Milan Kivala\*<sup>[a]</sup>

A  $\pi$ -expanded X-type double [5]helicene comprising dihydropyracylene moieties was synthesized from commercially available acenaphthene. X-ray crystallographic analysis revealed the unique highly twisted structure of the compound resulting in the occurrence of two enantiomers which were separated by chiral HPLC, owing to their high conformational stability. The compound shows strongly bathochromically shifted UV/vis absorption and emission bands with small Stokes shift and considerable photoluminescence quantum yield and circular

polarized luminescence response. The electrochemical studies revealed five facilitated reversible redox events, including three reductions and two oxidations, thus qualifying the compound as chiral multistage redox amphoteric. The experimental findings are in line with the computational studies based on density functional theory pointing towards increased spatial extension of the frontier molecular orbitals over the polycyclic framework and a considerably narrowed HOMO–LUMO gap.

## Introduction

Helicenes have attracted chemists for more than hundred years.<sup>[1]</sup> Owing to their unusual structural features helicenes initially belonged to the category of chemical curiosities, however, during the last decades their applicability in asymmetric catalysis,<sup>[2]</sup> molecular machines,<sup>[3]</sup> and liquid crystals<sup>[4]</sup> was successfully demonstrated. Recently, emission of circularly polarized light by  $\pi$ -expanded superhelicenes was shown.<sup>[5]</sup> Especially the incorporation of multiple helicene moieties within the same  $\pi$ -system affords interesting scaffolds with appealing

chiroptical properties.<sup>[6]</sup> Depending on the relative orientation of the helicene subunits around a common  $\pi$ -conjugated linker 'fused', 'crossed', and 'serial' polycyclic frameworks are distinguished.<sup>[7]</sup> Double helicenes are categorized as 'crossed' if they are fused at their central domain resulting in an X-shaped overall geometry. Although the first X-type double helicene **1** with two [5]helicene moieties attached to a common benzene core has already been reported back in 1959 (Figure 1),<sup>[8]</sup> further representatives such as **2** and **3** of this structurally appealing compound family still remain comparably scarce.<sup>[9]</sup> This situation is most likely owed to the fact that unsubstituted [5]helicenes generally possess relatively low energy barrier towards racemization,<sup>[10]</sup> preventing separation and chiroptical characterization of optically pure compounds. However, in all the hitherto reported cases the polycyclic scaffolds consist exclusively of benzenoid rings, while, to the best of our knowledge, compounds with odd-membered rings have not been reported to date. This is rather surprising, as for example  $\pi$ -conjugated cyclopentadiene moieties are known to readily undergo a facilitated electron uptake to give aromatic cyclo-

[a] Dr. J. Bergner, J. Borstelmann, C. Walla, Dr. F. Rominger, Prof. Dr. M. Kivala  
Organisch-Chemisches Institut  
Universität Heidelberg  
Im Neuenheimer Feld 270, 69120 Heidelberg (Germany)  
E-mail: milan.kivala@oci.uni-heidelberg.de

[b] L. M. Cavinato, J. P. Fuenzalida-Werner, Prof. Dr. R. D. Costa  
Technical University of Munich Campus Straubing  
Chair of Biogenic Functional Materials  
Schulgasse 22, 94315 Straubing (Germany)

[c] C. Walla, Prof. Dr. A. Dreuw  
Interdisziplinäres Zentrum für Wissenschaftliches Rechnen  
Universität Heidelberg  
Im Neuenheimer Feld 205 A, 69120 Heidelberg (Germany)

[d] H. Hinrichs, Dr. P. Schulze  
Abteilung Chromatographie & Elektrophorese  
Max-Planck-Institut für Kohlenforschung  
Kaiser-Wilhelm-Platz 1, 45470 Mülheim an der Ruhr (Germany)

Supporting information for this article is available on the WWW under <https://doi.org/10.1002/chem.202303336>

© 2023 The Authors. Chemistry - A European Journal published by Wiley-VCH GmbH. This is an open access article under the terms of the Creative Commons Attribution Non-Commercial NoDerivs License, which permits use and distribution in any medium, provided the original work is properly cited, the use is non-commercial and no modifications or adaptations are made.

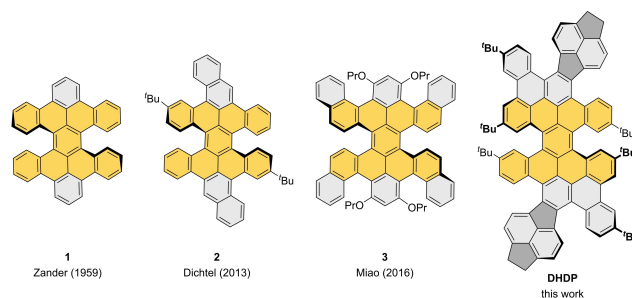


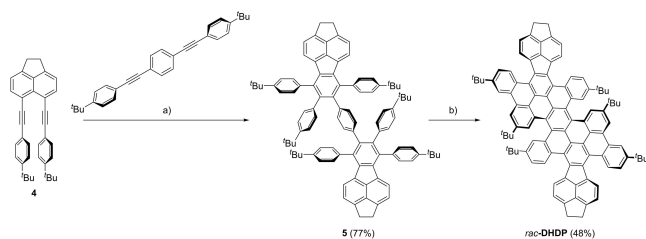
**Figure 1.** The evolution of X-type double [5]helicenes highlighted by the most relevant examples having a common benzene ring as the linking unit.

pentadienyl-like anions, thereby acting as reversible electron acceptors.<sup>[11]</sup>

Motivated by the electronic impact of the incorporated 5-membered rings we present herein the synthesis and characterization of  $\pi$ -expanded X-type double [5]helicene (DHDP) comprising two dihydropyracylene moieties.<sup>[12]</sup> The synthesized polycyclic framework is strategically decorated with <sup>t</sup>Bu groups to enhance the solubility, on the one hand, and, more importantly, to increase the steric demand and consequently to provide for conformational stability, on the other. Furthermore, the ethylene bridges of the dihydropyracylene moieties prevent the system from polymerization during the final cyclization step under oxidative conditions.<sup>[13]</sup> This strategy allowed for isolation of enantiomerically pure compounds and their chiroptical characterization.

## Results and Discussion

The key precursor compound **4** was synthesized from commercially available acenaphthene through a two-step sequence involving electrophilic bromination and a Sonogashira cross-coupling (for synthetic details, see the Supporting Information).<sup>[14]</sup> Oligophenylene **5** was obtained via a two-fold Rh-catalyzed [(2+2)+2] cyclotrimerization<sup>[15]</sup> of **4** with bis(4-*tert*-butylphenylethynyl)benzene in 77% yield upon heating in *o*-xylene (Scheme 1). The resulting beige solid of **5** was subjected



**Scheme 1.** Synthesis of *rac*-DHDP. a) Bis(4-*tert*-butylphenylethynyl)benzene, [RhCl(PPh<sub>3</sub>)<sub>3</sub>], *o*-xylene, 135 °C, N<sub>2</sub>, 52 h. b) DDQ, TfOH (1 v%), CH<sub>2</sub>Cl<sub>2</sub>, 0 °C, N<sub>2</sub>, 15 min. DDQ = 2,3-dichloro-5,6-dicyano-1,4-benzoquinone; TfOH = trifluoromethanesulfonic acid.

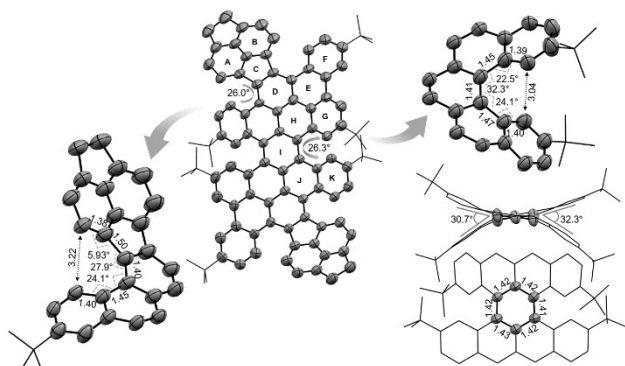


**Figure 2.** X-ray crystal structure of *rac*-DHDP (50% probability level, H-atoms and solvent molecules omitted, <sup>t</sup>Bu groups shown as wireframe for clarity). The most relevant structural parameters of the [5]helicene subunits and the central benzene ring are highlighted.

to a Brønsted acid-mediated cyclodehydrogenation with DDQ and triflic acid at 0 °C to achieve the desired *rac*-DHDP as red solid in 48% yield after HPLC. Other isomers were observed only in traces and could not be separated preparatively.

Single crystals of both the oligophenylene **5** and *rac*-DHDP suitable for X-ray crystallographic analysis were grown upon slow vapor diffusion of MeOH into a saturated solution of the compound in toluene (Figure 2 and the Supporting Information). An overall twisted structure is observed for *rac*-DHDP which is attributed to the steric hindrance induced by the adjacent <sup>t</sup>Bu groups strategically placed within the [5]helicene moieties (Figure 2). The helical pitch of both [5]helicene subunits, expressed as the distance between the '*ortho-ortho*' carbons, is in a range of 3.01–3.04 Å, which is in agreement with 2.93 Å reported for unsubstituted [5]helicene.<sup>[10]</sup> Compared to parent [5]helicene with the dihedral angle of 22.3°,<sup>[10]</sup> the respective mean values within the DHDP scaffold are slightly increased to 24.9° and 26.3°, which can be ascribed to the sterical hindrance of the <sup>t</sup>Bu groups. Moreover, the peripheral [5]helicene-like subunits involving the dihydropyracylene moieties are spanned wider in the solid state and the respective '*ortho-ortho*' carbon distances of 3.14–3.22 Å. As a result of the overall twisted geometry the central benzene ring (labeled I in Figure 2) acting as a common junction between the [5]helicene moieties appears distorted from its ideal hexagonal shape. While in precursor **5** no such distortion is observed (see the Supporting Information), the cyclization towards *rac*-DHDP leads to slight elongation of the C(sp<sup>3</sup>)–C(sp<sup>2</sup>) bonds by 0.02–0.04 Å (compared to benzene with 1.39 Å).<sup>[16]</sup> In addition, the carbon atoms of the benzene ring are located 0.01–0.15 Å above the mean plane. The dihedral angles within the benzene ring range from 11.1° to 25.3°, leading consequently to large bending angles of 30.7° and 32.3° (for definition, see the Supporting Information). Similar deformations of the benzene ring have been observed previously for example for the phosphorus-containing double helicene.<sup>[17]</sup>

*rac*-DHDP crystallizes as a racemic compound. As no other stereoisomers were found, it can be assumed that during the cyclization step both [5]helicenes are formed in a stepwise fashion. In this case, the chirality of the initially formed [5]helicene induces the stereochemistry of the second helical moiety during cyclization, leading to the formation of enantiomers rather than diastereomers. Analogous effects have been observed during the synthesis of other multiple helicenes previously.<sup>[18]</sup> The crystal packing of *rac*-DHDP is dictated by C(sp<sup>3</sup>)–H... $\pi$  interactions involving the dihydropyracylene moieties and occurring in a distance of about of about 3.75 Å. In addition, dispersion interactions between the <sup>t</sup>Bu groups are observed (see the Supporting Information).<sup>[19]</sup>

To assess the local aromaticity within the polycyclic framework of DHDP, nucleus independent chemical shift (NICS)<sup>[20]</sup> values were determined using the geometry optimized structure (Table 1 and the Supporting Information). While certain differences between the NICS(0) and NICS( $\pm$ 1) are found, reflecting the twisted geometry of the polycyclic framework, a distinct trend is clearly discernible. Thus, the rings of the peripheral naphthalene moiety (A and B in Figure 2) and the

| ring <sup>[a]</sup> | NICS(X) |       |       | HOMA  |
|---------------------|---------|-------|-------|-------|
|                     | -1      | 0     | +1    |       |
| A                   | -10.5   | -7.39 | -8.30 | +0.85 |
| B                   | -10.6   | -7.49 | -8.44 | +0.95 |
| C                   | +2.89   | +3.99 | +2.04 | -0.10 |
| D                   | -10.8   | -7.55 | -8.46 | +0.80 |
| E                   | -3.76   | +0.44 | -3.56 | +0.31 |
| F                   | -9.14   | -7.85 | -10.7 | +0.96 |
| G                   | -11.8   | -8.57 | -9.28 | +0.88 |
| H                   | -4.54   | +0.64 | -1.88 | +0.26 |
| I                   | -10.1   | -7.04 | -9.85 | +0.76 |
| J                   | -1.93   | +0.48 | -5.24 | +0.28 |
| K                   | -7.20   | -6.87 | -10.4 | +0.91 |

<sup>[a]</sup>Ring labels are assigned in Figure 2.

benzenoid rings with clearly assignable Clar  $\pi$ -electron sextets (D, F, G, I, and K) possess pronounced aromatic character, while the remaining 6-membered rings are basically non-aromatic. In contrast, the cyclopentadiene-like ring C is clearly antiaromatic. The harmonic oscillator model of aromaticity (HOMA) values as determined by using the atomic positions derived from X-ray crystallographic analysis of *rac*-DHDP nicely confirm the trends suggested by the NICS values.<sup>[21]</sup> The somewhat decreased NICS(0) and HOMA values of the central benzene ring I in DHDP of -7.04 and +0.76, respectively, compared to oligophenylene precursor **5** (-8.93 and +0.99; see the Supporting Information), nicely reflect the lowered aromaticity as a result of the geometrical distortion.

To gain insight into the optoelectronic properties, UV/vis spectroscopic analysis of **5** and *rac*-DHDP was performed in CH<sub>2</sub>Cl<sub>2</sub> at room temperature (Figure 3A and Table 2). The lowest energy absorption maximum of **5** is observed at 383 nm (accompanied by a shoulder at 399 nm), which is in line with the values reported for related fluoranthene derivatives.<sup>[22]</sup> Cyclization towards *rac*-DHDP shifts the lowest energy absorption bathochromically to 554 nm and leads to the occurrence of additional bands in the visible region. This observation corresponds to a narrowing of the optical band gap from 2.94 eV (for **5**) to 2.18 eV (for *rac*-DHDP), which is in line with the evolution of the HOMO and LUMO energies as revealed by

|          | $\lambda_{\max}$<br>[nm] | $\lambda_{\text{end}}$<br>[nm] | $E_{\text{g}}^{\text{opt}}$<br>[eV] <sup>[a]</sup> | $\lambda_{\text{em}}$<br>[nm] | Stokes<br>shift <sup>[b]</sup><br>[cm <sup>-1</sup> ] | $\Phi$ <sup>[c]</sup> | $E_{\text{red},3}^{\text{[d]}}$<br>[V] | $E_{\text{red},2}^{\text{[d]}}$<br>[V] | $E_{\text{red},1}^{\text{[d]}}$<br>[V] | $E_{\text{ox},1}^{\text{[d]}}$<br>[V] | $E_{\text{ox},2}^{\text{[d]}}$<br>[V] | HOMO <sup>[e]</sup><br>[eV] | LUMO <sup>[e]</sup><br>[eV] | $E_{\text{g}}^{\text{DFT}}$<br>[eV] |
|----------|--------------------------|--------------------------------|--|-------------------------------|---|-----------------------|--|--|--|---------------------------------------|---------------------------------------|-----------------------------|-----------------------------|-------------------------------------|
| <b>5</b> | 383                      | 422                            | 2.94   | 460                           | 4371  | 0.55                  | -                                      | -                                      | -2.39                                  | -                                     | -                                     | -5.40                       | -1.78                       | 3.62                                |
| DHDP     | 554                      | 570                            | 2.18   | 569                           | 476   | 0.43                  | -2.45                                  | -2.18                                  | -1.87                                  | +0.52                                 | +0.79                                 | -4.88                       | -2.25                       | 2.63                                |

<sup>[a]</sup>Calculated according to  $hc\lambda_{\text{end}}^{-1}$ ,  $\lambda_{\text{end}}$  estimated from the intersection of a tangent line to the lowest energy absorption band of the UV/vis spectrum with the x-axis. <sup>[b]</sup>Calculation of the Stokes shift by  $\lambda_{\text{em}} - \lambda_{\text{max}}$  and converted to wavenumbers. <sup>[c]</sup>Determined by using an integrating sphere. <sup>[d]</sup>Measured in THF and reported vs. Fc/Fc<sup>+</sup>. <sup>[e]</sup>DFT calculated values (B3LYP(D3BJ)/6-311G(d,p)).

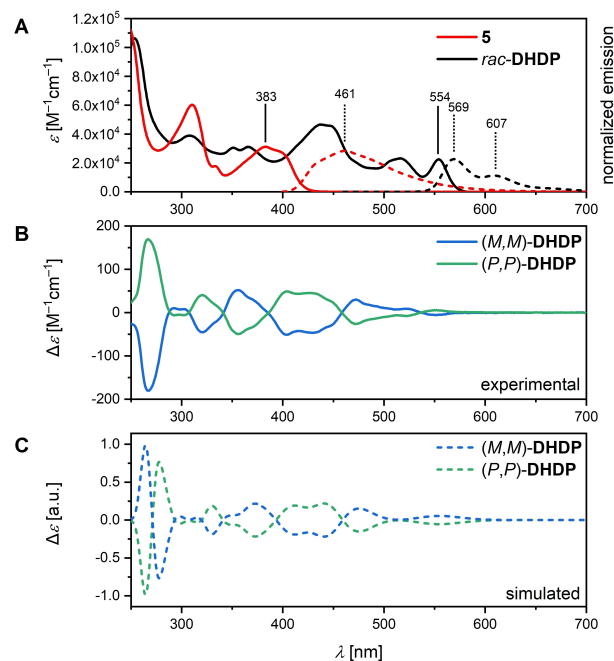


**Figure 3.** A: UV/vis absorption (full line) and emission (dashed line) spectra of **5** (red) and *rac*-DHDP (black). B: CD spectra of DHDP enantiomers (*M,M*)-DHDP (blue) and (*P,P*)-DHDP (green). All spectra were recorded in CH<sub>2</sub>Cl<sub>2</sub> at room temperature. C: Simulated CD spectra of the enantiomers (*M,M*)-DHDP (blue) and (*P,P*)-DHDP (green) by TD-DFT calculations at the B3LYP(D3BJ)/6-311G(d,p) level of theory. For better comparability, the simulated spectra are blueshifted by 0.04 eV.

DFT calculations at the B3LYP level of theory (Figure 5). Solutions of **5** and *rac*-DHDP in CH<sub>2</sub>Cl<sub>2</sub> show intense yellow to orange fluorescence. While the oligophenylene precursor **5** displays a single unstructured emission band at 461 nm with a Stokes shift of 4371 cm<sup>-1</sup>, *rac*-DHDP features vibronically structured emission with distinct maxima at 569 nm and 607 nm. The considerably smaller Stokes shift of 476 cm<sup>-1</sup> observed for *rac*-DHDP reflects the increased rigidity of the polycyclic framework. The corresponding PLQYs of 0.55 (for **5**) and 0.43 (for *rac*-DHDP) are remarkably high in comparison to other related polycyclic scaffolds comprising multiple helicene units.<sup>[6,7]</sup>

The promising spectroscopic features of *rac*-DHDP prompted us to separate its enantiomers by chiral HPLC for characterization of their chiroptical properties (for experimental details, see the Supporting Information). The circular dichroism

(CD) spectra recorded in  $\text{CH}_2\text{Cl}_2$  are perfect mirror images, supporting the occurrence of the respective enantiomers of **DHDP** (Figure 3B). By comparison of the experimental and simulated CD spectra at the B3LYP(D3BJ) level of theory with 6–311G(d,p) as basis set, the absolute configurations of the two enantiomers (*P,P*)-**DHDP** and (*M,M*)-**DHDP** were determined (Figure 3C).<sup>[23]</sup> The observed  $g_{\text{abs}}$  values are calculated to  $3.26 \times 10^{-3}$  at 272 nm and are, thus, in the range of the values reported for structurally related helical scaffolds.<sup>[7]</sup> Absorption of circularly polarized light is observed in the region from 250–570 nm and, thus, covers the whole UV/vis absorption. The conformational stability was investigated by heating a solution of the enantiopure (*M,M*)-**DHDP** in *n*-heptane to 60 °C for 4 h. Periodically recorded UV/Vis absorption and CD spectra showed no evidence of racemization or decomposition, allowing to estimate the lower limit of the energy barrier for racemization of 26.1 kcal mol<sup>-1</sup> at 333 K (see the Supporting Information).

Since organic emitters typically show a proportional relation between CD and circularly polarized luminescence (CPL),<sup>[24]</sup> CPL measurements were conducted to corroborate that the high degree of ground state chirality as documented by the CD spectra (Figure 3B) also translates into excited state chirality. Both enantiomers show only a weak CPL signal with  $g_{\text{lum}}$  values of about  $1 \times 10^{-3}$ , which is well in the range reported for other purely organic emitters (see the Supporting Information).<sup>[25]</sup>

To assess the evolution of the redox properties when going from oligophenylene **5** to *rac*-**DHDP** differential pulse voltammetry (DPV), cyclic voltammetry (CV) and square wave voltammetry (SWV) studies were conducted in THF (*n*-Bu<sub>4</sub>NPF<sub>6</sub> as supporting electrolyte (Figure 4 and Table 2). For precursor **5** only a single reversible reduction was observed at -2.39 V (vs. Fc/Fc<sup>+</sup>). In strong contrast, *rac*-**DHDP** shows three reversible reductions at -1.87 V, -2.18 V, and -2.45 V and two reversible oxidations at +0.52 V and +0.79 V. The occurrence of five reversible redox events for *rac*-**DHDP** clearly highlights the beneficial effect of cyclization on charge stabilization through efficient delocalization within the polycyclic framework. This is further supported by the DFT calculations pointing towards increased spatial extension of both the HOMO and the

LUMO with a concomitant dramatic narrowing of the HOMO–LUMO gap by 0.99 eV when going from oligophenylene **5** to cyclized *rac*-**DHDP** (Figure 5).<sup>[23]</sup>

## Conclusions

In summary, a new type of conformationally stable X-type double [5]helicene with dihydropyracylene moieties has been realized starting from commercially available acenaphthene. X-ray crystallographic analysis of the racemic compound confirmed the highly twisted molecular structure comprising two types of [5]helicene subunits. The strategic placement of <sup>t</sup>Bu groups provided for high conformational stability and separation of enantiomers by chiral HPLC which were characterized by chiroptical spectroscopy. Compared to the oligophenylene precursor the double helicene shows strongly bathochromically shifted UV/vis absorption and emission bands with small Stokes shift and considerable photoluminescence quantum yield. This observation indicates the progressive narrowing of the optical band gap and increased rigidity of the polycyclic framework. The double helicene undergoes five reversible redox events, including three reductions and two oxidations, which further showcases the beneficial effect of cyclization on charge stabilization by efficient delocalization within the polycyclic framework. These findings are further corroborated by computational studies based on density functional theory suggesting increased spatial extension of the frontier molecular orbitals and a significantly narrowed HOMO–LUMO gap. Our results overall identify the title compound as a new type of chiral fluorophore with multistage redox behavior and enhanced conformational stability.

## Experimental Section

Experimental details and characterization data for all compounds can be found in the Supporting Information. Deposition Numbers 2288649 (**S1**, for structure see the Supporting Information), 2288650 (**4**, for structure see the Supporting Information), and

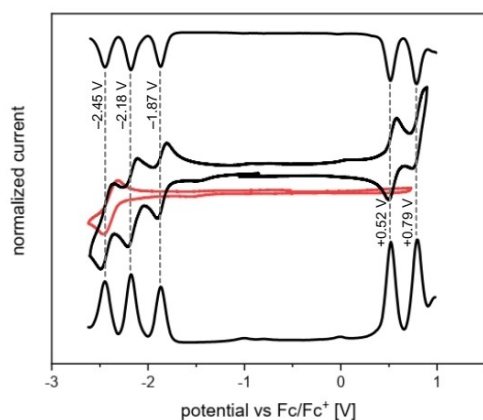


**Figure 4.** Electrochemistry of **5** (red) and *rac*-**DHDP** (black) (THF, *n*-Bu<sub>4</sub>NPF<sub>6</sub>, Fc/Fc<sup>+</sup>). Top: DPV; center: CV (scan rate 149 mVs<sup>-1</sup>); bottom: SWV.

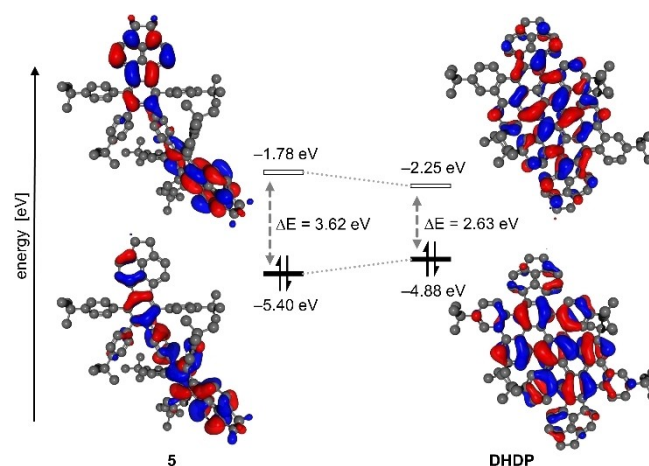


**Figure 5.** HOMO and LUMO of **5** and *rac*-**DHDP** (B3LYP(D3BJ)/6-311G(d,p)).<sup>[23]</sup>

2288651 (5, for structure see the Supporting Information), and 2288652 (*rac*-DHDP) contain the supplementary crystallographic data for this paper. The data can be obtained from The Cambridge Crystallographic Data Centre via Access Structures service.

## Supporting Information

The authors have cited additional references within the Supporting Information.<sup>[27–37]</sup>

## Acknowledgements

The generous funding by the Deutsche Forschungsgemeinschaft (DFG) – Project number 182849149-SFB 953 and Project number 281029004-SFB 1249 is acknowledged. Open Access funding enabled and organized by Projekt DEAL. L.M.C. and R.D.C. acknowledge the European Union's innovation under grant agreement MSCA-ITN STiBNite No. 956923. The authors acknowledge support by the state of Baden-Württemberg through bwHPC and the German Research Foundation (DFG) through grant no INST 40/575-1 FUGG (JUSTUS 2 cluster).

## Conflict of Interests

The authors declare no conflict of interest.

## Data Availability Statement

The data that support the findings of this study are available from the corresponding author upon reasonable request.

**Keywords:** double helicenes · [5]helicenes · chiroptical properties · conformational stability · pyracylene

- [1] a) M. Gingras, *Chem. Soc. Rev.* **2013**, *42*, 968; b) M. Gingras, G. Félix, R. Peresutti, *Chem. Soc. Rev.* **2013**, *42*, 1007; c) M. Gingras, *Chem. Soc. Rev.* **2013**, *42*, 1051.
- [2] M. T. Reetz, E. W. Beuttenmüller, R. Goddard, *Tetrahedron Lett.* **1997**, *38*, 3211.
- [3] a) T. R. Kelly, *Acc. Chem. Res.* **2001**, *34*, 514; b) T. B. Norsten, A. Peters, R. McDonald, M. Wang, N. R. Branda, *J. Am. Chem. Soc.* **2001**, *123*, 7447; c) K. Tanaka, H. Osuga, Y. Kitahara, *J. Org. Chem.* **2002**, *67*, 1795.
- [4] a) A. J. Lovinger, C. Nuckolls, T. J. Katz, *J. Am. Chem. Soc.* **1998**, *120*, 264; b) A. J. Lovinger, C. Nuckolls, T. J. Katz, *J. Am. Chem. Soc.* **1998**, *120*, 1944.
- [5] C. M. Cruz, S. Castro-Fernández, E. Maçóas, J. M. Cuerva, A. G. Campaña, *Angew. Chem. Int. Ed.* **2018**, *57*, 14782; *Angew. Chem.* **2018**, *130*, 14998.
- [6] Y.-F. Wu, L. Zhang, Q. Zhang, S.-Y. Xie, L.-S. Zheng, *Org. Chem. Front.* **2022**, *9*, 4726.
- [7] T. Mori, *Chem. Rev.* **2021**, *121*, 2373.
- [8] E. Clar, C. T. Ironside, M. Zander, *J. Chem. Soc.* **1959**, 142.
- [9] a) J. Luo, X. Xu, R. Mao, Q. Miao, *J. Am. Chem. Soc.* **2012**, *134*, 13796; b) H. Arslan, F. J. Uribe-Romo, B. J. Smith, W. R. Dichtel, *Chem. Sci.* **2013**, *4*, 3973; c) Y. Yang, L. Yuan, B. Shan, Z. Liu, Q. Miao, *Chem. Eur. J.* **2016**, *22*, 18620.
- [10] P. Ravat, R. Hinkelmann, D. Steinebrunner, A. Prescimone, I. Bodoky, M. Juriček, *Org. Lett.* **2017**, *19*, 3707.
- [11] a) J. D. Wood, J. L. Jellison, A. D. Finke, L. Wang, K. N. Plunkett, *J. Am. Chem. Soc.* **2012**, *134*, 15783; b) J. Bergner, C. Walla, F. Rominger, A. Dreuw, M. Kivala, *Chem. Eur. J.* **2022**, *28*, e202201554; c) S. Frisch, C. Neiß, S. Lindenthal, N. F. Zorn, F. Rominger, A. Görling, J. Zaumseil, M. Kivala, *Chem. Eur. J.* **2023**, *29*, e202203101.
- [12] Y.-H. Liu, D. F. Perepichka, *J. Mater. Chem. C* **2021**, *9*, 12448.
- [13] M. Wehmeier, M. Wagner, K. Müllen, *Chem. Eur. J.* **2001**, *7*, 2197.
- [14] a) R. Chinchilla, C. Najera, *Chem. Rev.* **2007**, *107*, 874; b) V. Vijay, R. Ramakrishnan, M. Hariharan, *Cryst. Growth Des.* **2021**, *21*, 200.
- [15] a) Y.-T. Wu, T. Hayama, K. K. Baldrige, A. Linden, J. S. Siegel, *J. Am. Chem. Soc.* **2006**, *128*, 6870; b) Y. Shibata, K. Tanaka, *Synthesis* **2012**, *44*, 323.
- [16] G. A. Jeffrey, J. R. Ruble, R. K. McMullan, J. A. Pople, *Proc. R. Soc. London Ser. A* **1987**, *414*, 47.
- [17] S. Hashimoto, S. Nakatsuka, M. Nakamura, T. Hatakeyama, *Angew. Chem. Int. Ed.* **2014**, *53*, 14074; *Angew. Chem.* **2014**, *126*, 14298.
- [18] a) F. Zhang, E. Michail, F. Saal, A.-M. Krause, P. Ravat, *Chem. Eur. J.* **2019**, *25*, 16241; b) S. Ma, J. Gu, C. Lin, Z. Luo, Y. Zhu, J. Wang, *J. Am. Chem. Soc.* **2020**, *142*, 16887; c) R. K. Dubey, M. Melle-Franco, A. Mateo-Alonso, *J. Am. Chem. Soc.* **2022**, *144*, 2765.
- [19] J. P. Wagner, P. R. Schreiner, *Angew. Chem. Int. Ed.* **2015**, *54*, 12274; *Angew. Chem.* **2015**, *127*, 12446.
- [20] Z. Chen, C. S. Wannere, C. Corminboeuf, R. Puchta, P. v. R. Schleyer, *Chem. Rev.* **2005**, *105*, 3842.
- [21] T. M. Krygowski, M. K. Cyrański, *Chem. Rev.* **2001**, *101*, 1385.
- [22] N. D. Marsh, C. J. Mikolajczak, M. J. Wornat, *Spectrochim. Acta Part A* **2000**, *56*, 1499.
- [23] a) P. Hohenberg, W. Kohn, *Phys. Rev.* **1964**, *136*, B864-B871; b) W. Kohn, L. G. Sham, *Phys. Rev.* **1965**, *140*, A1133-A1138; c) C. Lee, W. Yang, R. G. Parr, *Phys. Rev. B* **1988**, *37*, 785; d) A. D. Becke, *J. Chem. Phys.* **1993**, *98*, 5648; e) S. Grimme, J. Antony, S. Ehrlich, H. Krieg, *J. Chem. Phys.* **2010**, *132*, 154104; f) S. Grimme, S. Ehrlich, L. Goerigk, *J. Comput. Chem.* **2011**, *32*, 1456.
- [24] H. Tanaka, Y. Inoue, T. Mori, *ChemPhotoChem* **2018**, *2*, 386.
- [25] a) L. Arrico, L. Di Bari, F. Zinna, *Chem. Eur. J.* **2021**, *27*, 2920; b) E. M. Sánchez-Carnerero, A. R. Agarrabeitia, F. Moreno, B. L. Maroto, G. Muller, M. J. Ortiz, S. de La Moya, *Chem. Eur. J.* **2015**, *21*, 13488.
- [26] Deposition Numbers 2288649 (S1, for structure see the Supporting Information), 2288650 (4), 2288651 (5) and 2288652 (DHDP) contain the supplementary crystallographic data for this paper. The data can be obtained free of charge from The Cambridge Crystallographic Data Centre Access Structures service.
- [27] G. R. Fulmer, A. J. M. Miller, N. H. Sherden, H. E. Gottlieb, A. Nudelman, B. M. Stoltz, J. E. Bercaw, K. I. Goldberg, *Organometallics* **2010**, *29*, 2176.
- [28] G. M. Sheldrick, *Acta Crystallogr. Sect. A* **2008**, *64*, 112.
- [29] G. M. Sheldrick, *Acta Crystallogr. Sect. C* **2015**, *71*, 3.
- [30] C. F. Macrae, P. R. Edgington, P. McCabe, E. Pidcock, G. P. Shields, R. Taylor, M. Towler, J. van de Streek, *J. Appl. Crystallogr.* **2006**, *39*, 453.
- [31] a) E. Epifanovsky, A. T. B. Gilbert, X. Feng, J. Lee, Y. Mao, N. Mardirossian, P. Pokhilko, A. F. White, M. P. Coons, A. L. Dempwolff, Z. Gan, D. Hait, P. R. Horn, L. D. Jacobson, I. Kaliman, J. Kussmann, A. W. Lange, K. U. Lao, D. S. Levine, J. Liu, S. C. McKenzie, A. F. Morrison, K. D. Nanda, F. Plasser, D. R. Rehn, M. L. Vidal, Z.-Q. You, Y. Zhu, B. Alam, B. J. Albrecht, A. Aldossary, E. Alguire, J. H. Andersen, V. Athavale, D. Barton, K. Begam, A. Behn, N. Bellonzi, Y. A. Bernard, E. J. Berquist, H. G. A. Burton, A. Carreras, K. Carter-Fenk, R. Chakraborty, A. D. Chien, K. D. Closser, V. Cofer-Shabica, S. Dasgupta, M. de Wergifosse, J. Deng, M. Diedenhofen, H. Do, S. Ehlert, P.-T. Fang, S. Fatehi, Q. Feng, T. Friedhoff, J. Gayvert, Q. Ge, G. Gidofalvi, M. Goldey, J. Gomes, C. E. González-Espinoza, S. Gulania, A. O. Gunina, M. W. D. Hanson-Heine, P. H. P. Harbach, A. Hauser, M. F. Herbst, M. Hernández Vera, M. Hodecker, Z. C. Holden, S. Houck, X. Huang, K. Hui, B. C. Huynh, M. Ivanov, Á. Jász, H. Ji, H. Jiang, B. Kaduk, S. Kähler, K. Khistyayev, J. Kim, G. Kis, P. Klunzinger, Z. Koczor-Benda, J. H. Koh, D. Kosenkov, L. Koulias, T. Kowalczyk, C. M. Krauter, K. Kue, A. Kunitas, T. Kus, I. Ladžánszki, A. Landau, K. V. Lawler, D. Lefrançois, S. Lehtola, R. R. Li, Y.-P. Li, J. Liang, M. Liebenthal, H.-H. Lin, Y.-S. Lin, F. Liu, K.-Y. Liu, M. Loipersberger, A. Luenser, A. Manjanath, P. Manohar, E. Mansoor, S. F. Manzer, S.-P. Mao, A. V. Marenich, T. Markovich, S. Mason, S. A. Maurer, P. F. McLaughlin, M. F. S. J. Menger, J.-M. Mewes, S. A. Mewes, P. Morgante, J. W. Mullinax, K. J. Oosterbaan, G. Parani, A. C. Paul, S. K. Paul, F. Pavošević, Z. Pei, S. Prager, E. I. Proynov, Á. Rák, E. Ramos-Cordoba, B. Rana, A. E. Rask, A. Rettig, R. M. Richard, F. Rob, E. Rossomme, T. Scheele, M. Scheurer, M. Schneider, N. Sergueev, S. M. Sharada, W. Skomorowski, D. W. Small, C. J. Stein, Y.-C. Su, E. J. Sundstrom, Z. Tao, J. Thirman, G. J. Tornai, T. Tsuchimochi, N. M.

- Tubman, S. P. Veccham, O. Vydrov, J. Wenzel, J. Witte, A. Yamada, K. Yao, S. Yeganeh, S. R. Yost, A. Zech, I. Y. Zhang, X. Zhang, Y. Zhang, D. Zuev, A. Aspuru-Guzik, A. T. Bell, N. A. Besley, K. B. Bravaya, B. R. Brooks, D. Casanova, J.-D. Chai, S. Coriani, C. J. Cramer, G. Cserey, A. E. DePrince, R. A. DiStasio, A. Dreuw, B. D. Dunietz, T. R. Furlani, W. A. Goddard, S. Hammes-Schiffer, T. Head-Gordon, W. J. Hehre, C.-P. Hsu, T.-C. Jagau, Y. Jung, A. Klamt, J. Kong, D. S. Lambrecht, W. Liang, N. J. Mayhall, C. W. McCurdy, J. B. Neaton, C. Ochsenfeld, J. A. Parkhill, R. Peverati, V. A. Rassolov, Y. Shao, L. V. Slipchenko, T. Stauch, R. P. Steele, J. E. Subotnik, A. J. W. Thom, A. Tkatchenko, D. G. Truhlar, T. van Voorhis, T. A. Wesolowski, K. B. Whaley, H. L. Woodcock, P. M. Zimmerman, S. Faraji, P. M. W. Gill, M. Head-Gordon, J. M. Herbert, A. I. Krylov, *J. Chem. Phys.* **2021**, *155*, 84801; b) T. Yanai, D. P. Tew, N. C. Handy, *Chem. Phys. Lett.* **2004**, *393*, 51.
- [32] a) V. Barone, M. Cossi, *J. Phys. Chem. A* **1998**, *102*, 1995; b) M. Cossi, N. Rega, G. Scalmani, V. Barone, *J. Comput. Chem.* **2003**, *24*, 669.
- [33] Roy Dennington, Todd A. Keith, John M. Millam, GaussView Version 6 2019.
- [34] S. Ma, J. Gu, C. Lin, Z. Luo, Y. Zhu, J. Wang, *J. Am. Chem. Soc.* **2020**, *142*, 16887.
- [35] N. Tanaka, T. Kasai, *Bull. Chem. Soc. Jpn.* **1981**, *54*, 3020.
- [36] a) C. L. Eversloh, Z. Liu, B. Müller, M. Stangl, C. Li, K. Müllen, *Org. Lett.* **2011**, *13*, 5528; b) G. Schoetz, O. Trapp, V. Schurig, *Electrophoresis* **2001**, *22*, 3185.
- [37] A. Behn, P. M. Zimmerman, A. T. Bell, M. Head-Gordon, *Chem. Phys.* **2011**, *135*, 224108.

---

Manuscript received: November 12, 2023

Accepted manuscript online: November 20, 2023

Version of record online: December 14, 2023